Karakterisatie en testen van 'thin film nanocomposite' en 'thin film composite' RO membranen

BTO 2012.230(s)
November 2012

Watercycle Research Institute

KWR Watercycle Research Institute

Karakterisatie en testen van 'thin film nanocomposite' en 'thin film composite' RO membranen

BTO 2012.230(s)
November 2012

Postbus 1072 3430 BB Nieuwegein T 030 606 95 11 F 030 606 11 65 E info@kwrwater.nl I www.kwrwater.nl

Colofon

Titel
Karakterisatie en testen van 'thin film nanocomposite' en 'thin film composite' RO membranen

Opdrachtnummer
B111679

Rapportnummer
BTO 2012.230(s)

Onderzoeksprogramma
Waterbehandeling

Projectmanager
E.F. Beerendonk

Opdrachtgever
CvO

Kwaliteitsborger
J.W. Post

Auteurs
B. Hofs, R. Schurer (Evides), D.J.H. Harmsen, C. Ceccarelli, E.F. Beerendonk, E.R. Cornelissen

Verzonden aan
PBC Waterbehandeling

Dit rapport is selectief verspreid onder medewerkers van BTO-participanten.

Voorwoord

Dit rapport bestaat uit een (ingediend) Engelstalig artikel en een Nederlandstalige samenvatting daarvan. Het onderzoek dat in dit rapport wordt beschreven is uitgevoerd in samenwerking met Evides. Het eerste deel van het onderzoek is uitgevoerd bij KWR (uitgevoerd door stagiair Chloé Ceccarelli [1]), en het tweede deel bij Evides (zeewaterontzoutingpilot Kamperland).

Samenvatting

Samenvatting behorende bij het artikel 'Characterization and performance of a commercial thin film nanocomposite seawater reverse osmosis membrane' (zie hoofdstuk 1)

Inleiding

In 2009 werd het bedrijf NanoH_2O binnen het BTO geselecteerd als een van de meest kansrijke start-ups met een product gebaseerd op nanotechnologie [2]. Eind 2011 is NanoH_2O met een nieuw uniek (zeewaterontzoutings)membraan op de markt gekomen van het type 'thin film nanocomposite' (TFN) waarbij nanodeeltjes in de actieve laag zijn bereid. De grootste belofte van het TFN membraan ten opzichte van conventionele thin film composite (TFC) membranen was een verhoogde permeabiliteit voor water bij gelijkblijvende zoutretentie: daarmee zou zeewater met een 40% lager energieverbruik ontzout kunnen worden.

In het kader van het in het BTO lopende onderzoek naar nanotechnologie zijn de TFN membranen vergeleken met conventionele TFC membranen, zowel in testbankonderzoek bij KWR als in langlopende pilottesten met zeewaterontzouting bij Evides (vanaf begin 2012 tot medio 2012). De gebruikte conventionele membranen zijn relatief dichte TFC membranen met een lage zout- en waterpermeabiliteit.

Doel en uitvoering

De TFN membranen zijn vergeleken met een standaard TFC zeewaterontzoutingsmembranen van Dow Filmtec. De oppervlakte-eigenschappen van beide membranen zijn bepaald met scanning electron microscopy with energy dispersive X-ray spectroscopy (SEM-EDX) (bepaling aanwezige atomen) en uitgebreide contacthoek-, en zeta-potentiaalmetingen (respectievelijk bepaling hydrophobiciteit en lading). In testbankonderzoek (Foto's 1, voeding 0,2 m^3/h) zijn de prestaties van beide membranen (4040 elementen – 40 inch lengte, Ø 4,0 inch) vergeleken met betrekking tot de water-, en zoutpermeabiliteit en retentie voor zouten, glycerol en nitrosoamines bij een flux van rond de 15 L m^{-2} h^{-1} en een lage recovery (rond de 7,5%).

Daarnaast zijn in een (zeewaterontzouting)pilottest bij Evides de prestaties vergeleken van beide membranen met betrekking tot flux, zout-, en boorretentie. Hiervoor is één van de vijf drukbuizen in de zeewaterontzoutingpilotinstallatie van Evides (Foto's 2, voeding 37,5 m^3/h) gevuld met zes TFN membranen (8040 elementen - 80 inch lengte, Ø 4,0 inch). In de andere drukbuizen zaten sinds begin 2009 membranen van het TFC type. Van januari 2012 tot eind juli 2012 zijn daarbij de flux en zout-, en boorretentie van de beide types membranen bepaald. De flux bij deze testen varieerde rond de 15 L m^{-2} h^{-1} en de recovery rond de 40%.

Resultaten en discussie

Er zit weinig verschil tussen de oppervlakte-eigenschappen van de membranen gelet op de SEM-EDX analyse en de contacthoek-, en zeta-potentiaalmetingen. Het TFN membraan is iets hydrofober dan het TFC membraan, maar de lading en de compositie (qua aanwezige elementen) zijn gelijk. De in de TFN gebruikte nanodeeltjes zijn met de EDX analyse niet terug te vinden; ze zijn waarschijnlijk in een te lage concentratie (<6%) aanwezig.

Uit testbankexperimenten met de 4040 elementen blijkt dat de waterpermeabiliteit van de TFN bijna twee keer zo hoog is als die van de TFC, terwijl ze beiden ongeveer dezelfde zoutpermeabiliteit hebben (NaCl). De TFN heeft echter wel een lagere retentie voor glycerol en NDMA dan de TFC.

Uit experimenten bij Evides (zes 8040 elementen per drukbuis) blijkt ook dat de TFN membranen een bijna dubbele productie hebben, vergeleken met de TFC membranen. De zoutretentie van de TFC membranen is iets hoger dan die van de TFN membranen. Vooral het verschil tussen de TFN en TFC membranen in boorretentie valt op. In het permeaat van de drukbuis met TFN membranen zat gemiddeld 1,2 mg/L boor, terwijl in het permeaat van de drukbuizen met TFC membranen gemiddeld slechts 0,53 mg/L boor zat. In de EU is de toegestane hoeveelheid boor in drinkwater 1 mg/L. Aangezien de retentie ook sterk afhangt van de watertemperatuur, betekent dit dat het permeaat van de TFN membranen voor een gedeelte van het jaar niet aan de eisen zou voldoen, waardoor er extra behandeling nodig is. Hiervoor zijn meerdere mogelijke oplossingen te bedenken; bijvoorbeeld het

nabehandelen van het permeaat met RO, of het bijmengen van (drink)water met een veel lager boorgehalte.
Bij deze vergelijking tussen TFC en TFN membranen is het goed om te weten dat NanoH$_2$O in 2012 met nieuwe membranen op de markt is gekomen die een hogere boorretentie hebben dan de hier geteste TFN. Deze membranen hebben we nog niet kunnen testen, maar ze hebben volgens de opgegeven specificaties een vergelijkbare waterpermeabiliteit als de hier geteste TFC membranen. Daarnaast zijn er ook TFC membranen beschikbaar, die een bijna net zo hoge waterpermeabiliteit hebben als de hier geteste TFN membranen. Voor deze TFC membranen geldt dat de retentie voor zouten lager is dan voor de dichtere hier geteste TFC membranen.

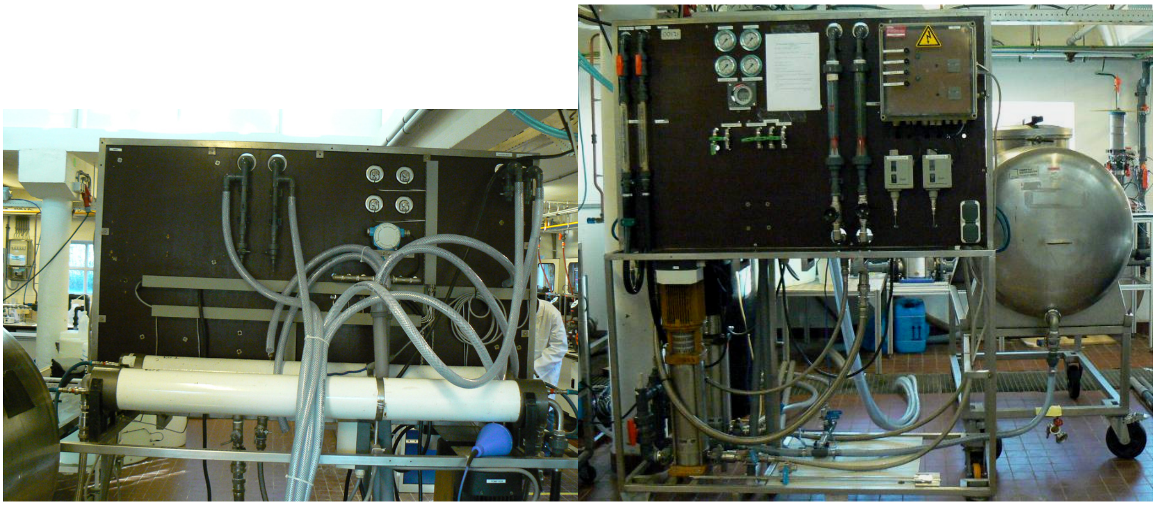
Foto's 1: De dubbelloopspilot van KWR.
Links: Achterzijde met beide drukbuizen zichtbaar.
Rechts: Voorzijde, met aan de rechterkant de recirculatietank.


Foto's 2: De zeewaterontzoutingpilot van Evides.
Links: SWRO installatie met hoge druk pomp en vijf drukbuizen met zes 8040 elementen per drukbuis.
Rechts: concentraatzijde, met onderaan het monsterpunt voor het concentraat van de onderste drukbuis met de NanoH$_2$O elementen.

Conclusie en vooruitzicht

Het hier geteste TFN membraan heeft een hogere waterpermeabiliteit dan de geteste TFC membranen. De retentie van zouten en organische microverontreinigingen is echter iets lager voor het TFN membraan dan voor het TFC membraan.

Er zijn echter ondertussen nieuwe TFN membranen op de markt gekomen, waarvan de waterpermeabiliteit en zoutretentie meer overeenkomt met de TFC membranen. Daarmee kan geconcludeerd worden dat de huidige generatie TFN en TFC membranen vergelijkbare prestaties leveren. De toevoegde nanodeeltjes in de actieve laag van het TFN membraan zijn niet gedetecteerd (waarschijnlijk <6% aanwezig); daarmee lijkt het logisch dat de prestaties van de TFN membranen vergelijkbaar zijn met die van TFC membranen.

De belofte van de TFN membranen is met de eerste generatie producten niet helemaal waargemaakt (dubbele opbrengst, dezelfde retentie), maar wat niet is, kan nog komen.

Referenties bij voorwoord en samenvatting

[1] Ceccarelli, C., DWB-2012-02-CC (intern rapport), OMPs rejection by virgin and biofouled membranes, KWR

[2] Hofs, B., BTO 2009.023(s), Literatuuronderzoek Nanotechnologie voor waterbehandeling, KWR

Inhoud

1 Characterization and performance of a commercial thin film nanocomposite seawater reverse osmosis membrane

B. Hofs[1]*, R. Schurer[2], D.J.H. Harmsen[1], C. Ceccarelli[1], E.F. Beerendonk[1], E.R. Cornelissen[1]
[1] *KWR Watercycle Research Institute, P.O. Box 1072, 3430 BB Nieuwegein, The Netherlands*
*corresponding author, *e-mail: bas.hofs@kwrwater.nl, telephone: (+31)(0)306069697, fax:(+31)(0)306061165*
[2] *Evides Water Supply Company, Berenplaat 10, 3207 LB Spijkenisse, The Netherlands*

1.1 Abstract

The properties and performance of a recently developed thin film nanocomposite (TFN), with inorganic nanoparticles incorporated in the active layer, and standard thin film composite (TFC) spiral wound seawater desalination reverse osmosis (RO) membranes were assessed by comparison on the scale of 4040 and 8040 membrane modules.

Scanning electron microscopy with energy-dispersive X-ray spectroscopy, contact angle-, and ζ-potential measurements did not show large differences between TFN membranes and a commercial TFC membrane. Small scale pilot tests (4040 elements) showed that the TFN had a factor two higher water permeability as the TFC. Salt rejection was the same, but the TFC showed slightly better rejection of NDMA and glycerol. Larger scale pilot tests (multiple 8040 elements) confirmed the nearly twofold higher water permeability for the TFN as compared aged TFC membranes. However, the boron rejection of the TFN was lower than that of the aged TFC.

Keywords: thin film composite, desalination, salt rejection, micro-pollutants, SWRO

1.2 Highlights

> A TFN membrane shows nearly a factor 2 higher water permeability than a standard TFC
> A standard TFC membrane shows better rejection of glycerol and NDMA than a TFN
> TFN membrane boron rejection is lower than that of a standard TFC
> The current generation of TFNs and TFCs show comparable performances

1.3 Introduction

Since the start of seawater desalination with reverse osmosis (RO) membranes, RO membranes have been extensively developed towards greater water permeability whilst also maintaining or even enhancing the rejection of salts [1]. The commercially most successful RO membranes in current use are thin film composites, with a typical three layer structure. The thin (in the order of 100 nm thickness) dense active membrane layer (the 'thin film') is attached to a more open and thicker intermediate layer (about 40 µm), which is attached to an even more open support layer [1]. The properties of the thin film largely determine the clean membrane resistance. A potentially new generation of RO desalination membranes, thin film nano-composite (TFN) RO membranes, was developed recently [2, 3]. Unlike other new potential types of desalination membranes [1], like those proposed with graphene oxide sheets [4], carbon nanotubes [5] or aquaporins [6] as the active membrane layer, however, the TFN membrane is already commercially available. In the TFN membranes investigated in literature Linde type A zeolite particles of varying size are embedded in the thin film in order to enhance the water permeability [7, 8]. The zeolite particles size (around 100 nm) and their internal structure, is such that they may potentially be called nanotechnology. Larger zeolite particles are more effective in increasing the permeability, but greatly decrease the rejection [7]. Seawater can be desalinated with these type of membranes, as was shown recently [8], although the boron rejection was not measured. The commercially available TFN RO membranes (type of nanoparticles used not disclosed) are stated to have a 50-100% increased water permeability when compared to the installed base of seawater RO (SWRO) membranes, whilst having a similar salt rejection [9]. Besides the water permeability and salt rejection, the boron rejection of SWRO membranes is important. In a recent study on the boron rejection of full scale desalination plants performed for the U.S. Department of the Interior, Bureau of Reclamation [10], it was found that the observed boron rejection in full scale plants was 65-80% (substantially lower than measured in lab-scale experiments [10, 11]). For some full scale plants the European Communities Drinking Water Regulations [12] and California Department of Health Services action level [13] of 1 mg/L boron was only just reached [10], but the World Health Organization (WHO) guidelines for drinking water state that boron concentrations in drinking water of 2.4 mg/L [14] was reached easily in all full scale plants [10]. Note that the required level of boron in the finished product varies in different countries may be anywhere between 0.3 (Israel) and 5 mg/L (Canada) [11].

The occurrence and removal of organic micro-pollutants has received a lot of attention in recent literature (see [15-20] and references therein). For membrane processes, like nanofiltration (NF) and RO, the removal of organic micro-pollutants depends primarily on the effective size of the organic micro-pollutants and the molecular weight cut-off (MWCO) of the membranes, and secondarily on the charge and hydrophobicity of both organic micro-pollutants and membranes (see [21, 22] and references therein). It is expected that with increasing anthropogenic impact on the environment and especially surface waters, these types of compounds will increasingly need to be removed in drinking water treatment.

In this paper we characterize and investigate the performance of a commercially available TFN RO membrane, compared to that of a standard thin film composite (TFC) commercial RO membrane. The flux, and the rejection of salt, glycerol and various micro-pollutants of a TFC and TFN membrane are measured and compared on a small pilot scale. The micro-pollutants studied are a set of nitrosamines and a set of pharmaceuticals. The flux and rejection of salt (including boron) of a TFC and TFN membrane are measured and compared for a larger scale pilot plant as well.

1.4 Materials and methods

1.4.1 Chemicals

NaCl, glycerol, diiodomethane, the used 21 pharmaceuticals (atenolol, bezafibraat, carbamazepine, clenbutarol, clofibrinezuur, cyclophosphamide, diclofenac, gemfibrozil, ketoprofen, metformin, metoprolol, naproxen, paracetamol, pentoxifylline, pindolol, propranolol, salbutamol, sotalol, sulfamethoxazole, terbutaline and trimethoprim) and eight nitrosoamines (see Table 1), were obtained from respectable commercial sources in high purity (typically >98%) and used as received.

1.4.2 Analysis

Concentrations of chloride, sulphate, ammonium, nitrate and fluoride were determined by Vitens Laboratory Utrecht (Utrecht, The Netherlands). Sodium chloride (and other salts) concentrations were determined quantitatively with inductively coupled plasma mass spectrometry (ICP-MS) at the KWR laboratory (Nieuwegein, The Netherlands) following an in-house procedure (LAM-058). All other (see table 1) measurements were performed at the KWR laboratory, with in-house methods or text-book procedures (pH: in accordance with NEN-ISO 10523, hydrogen carbonate: by titration with acid, in-house method LAM-042, electrical conductivity: measured with a CDM 83 conductivity meter (Radiometer, conforming to ISO 7888, at 25 °C)).

The concentrations of glycerol were determined by measuring the non-purgeable organic carbon (NPOC) content with in-house method LAM-041, in accordance with ISO 8245 and NENEN 1484. This method has a detection limit of about 0.1 mg/L.

The concentrations of the 21 pharmaceuticals were determined with direct injection and ultra performance liquid chromatography coupled with a mass spectrometer (UPLC-MS/MS) with in-house method LOA-548. The method is composed of two separate UPLC-MS/MS measurements; one based on reversed phase (RP) chromatography, and one on “hydrophilic interaction chromatography” (HILIC) for the very polar compound (metformin). The used mass spectrometer is a triple quadrupole mass spectrometer with electrospray interface (TSQ Vantage). The limit of quantification (LOQ) for the pharmaceuticals was 10 ng/L, except for metformin which had a LOQ of 50 ng/L.

The concentrations of the eight nitrosamines (see table 1) were determined by extraction from the water phase with solid phase extraction (SPE) and subsequent analysis with capillary gas chromatography

combined with mass spectrometry (GC-MS) and chemical ionization aided by ammonia (CI) (in-house method CI+: LOA-535). The LOQ for the various nitrosamines varied from 20 to 60 ng/L.
A select set of deuterated internal standards was used in both methods (LOA-548 and LOA-545). The concentration of both pharmaceuticals and nitrosamines was calculated using an external calibration curve, and corrected for the applied internal standard.

Table 1: Properties of the used nitrosoamines and glycerol

compound	abbreviation	CAS number	Molecular weight (MW, in g/mol)	molecular formula
glycerol		56-81-5	96.1	$C_3H_8O_3$
N-nitrosodimethylamine	NDMA	62-75-9	74.1	$C_2H_6N_2O$
N-nitrosomethylethylamine	NMEA	10595-95-6	88.1	$C_3H_8N_2O$
N-nitrosopyrrolidine	NPYR	930-55-2	100	$C_4H_8N_2O$
N-nitrosodiethylamine	NDEA	55-18-5	102	$C_4H_{10}N_2O$
N-nitrosopiperidine	NPIP	100-75-4	114	$C_5H_{10}N_2O$
N-nitrosomorpholine	NMOR	59-89-2	118	$C_4H_8N_2O_2$
N-nitrosodi-n-propylamine	NDPA	621-64-7	130	$C_6H_{14}N_2O$
N-nitroso-n-dibutylamine	NDBA	924-16-3	158	$C_8H_{18}N_2O$

1.4.3 Membranes

1.4.3.1 Properties

The following membranes were obtained (directly or indirectly) from the manufacturers: QuantumFlux (Qfx) SW 75ES RO membranes from NanoH_2O (El Segundo, California, USA), which are TFN membranes with inorganic nanoparticles, and Filmtec SW30HRLE 4040 units via Lenntech (Delft, The Netherlands), which are standard TFC membranes. Both these membranes are standard spiral wound 4 inch elements. The membrane properties are given in table 2.
The 8 inch membranes were obtained from the manufacturers: QuantumFlux (Qfx) SW 365ES RO membranes from NanoH_2O (El Segundo, California, USA) and Filmtec SW30XHR-440i units from Dow Filmtec. Both these membranes are standard spiral wound 8 inch elements. A selection of membrane properties (area, flux, surface roughness, contact angle of water, ζ-potential, the stabilized NaCl rejection and the permeate production under standardized test conditions) is given in table 2.

Table 2: Membrane properties

	SW30HRLE	Qfx SW 75ES	SW30XHR-440i	QFX 365 ES	unit
Area	7.9[2]	7.0[2]	41[2]	34[2]	m^2
Flux[7]	32[2,3]	58[2]	25[2]	58[2]	$L\ m^{-2}\ h^{-1}$
Surface roughness[1]	100[3,4]				nm
Contact angle (water)	33 to 47[3,4]				°
ζ-potential	-15 to -33[3,5,6]				mV
Stabilized NaCl rejection	99.75[2]	99.75[2]	99.82[2]	99.8[2]	%
Production[7]	31	47	25		m^3/day

[1] Surface roughness, expressed as root mean squared (RMS) surface roughness as determined by atomic force microscopy (AFM) in listed references

[2] Information supplied by the manufacturer (product sheets)

[3] [23]

[4] [24]

[5] [25]

[6] [26]

[7] Flux and production of a single 4040 element under standardized testing conditions at P_f = 55 bar, according to information supplied by the manufacturer (product sheets)

1.4.3.2 Characterization

1.4.3.2.1 Membrane performance

The water and salt permeability constants (A and B, respectively - [27, 28]) were determined from experiments as described in §2.5. The *U*, *n* and *m* constants [29] which are part of the temperature correction factors (TCF) and the capacity correction factor (QCF) were determined as well. The following equations were used with the correction factors:

$$TCF_A = e^{U\left(\frac{1}{Ta}-\frac{1}{Tr}\right)} \tag{1}$$

where *U* is the correction factor for temperature, and determines temperature effects on A.

$$TCF_{\Delta P} = (\eta_{Tr}/\eta_{Ta})^n \tag{2}$$

where η is the viscosity at the reference or actual temperature (T_r and T_a, respectively) and *n* is the correction factor for the temperature which determines temperature effects on the pressure drop ΔP.

$$QCF_{\Delta P} = \left(\frac{Q_r}{(Q_f + Q_c)/2}\right)^m \tag{3}$$

where Q_r is the reference (feed and concentrate) flow, Q_f the actual feed flow, Q_c the actual concentrate flow and *m* is the correction factor for the flow and the flow effects on ΔP.

2.3.2.2 Contact angle measurements

Contact angle measurements (CAM) were carried out to calculate the surface tensions components ($\gamma_M^{LW}, \gamma_M^+, \gamma_M^-$, see below) of the membranes and the free energy of interaction (ΔG_i) between the solute and the membrane in a liquid [30]. The membranes were cut into small pieces (5*5 cm^2) and these pieces were used to measure the contact angle of three liquids (water, glycerol and diiodomethane). Ten drops of each liquid were deposited on the membranes and the contact angle of each drop was measured using a Krüss DSA10 goniometer (Krüss GmbH, Hamburg, Germany) with matching software (Drop Shape Analysis, version 1.9). γ's and ΔG were calculated as described elsewhere [30]. The surface tension components were determined with the Young-Dupré equation [31];

$$(1+\cos\theta)\gamma_L = 2(\sqrt{\gamma_M^{LW}\gamma_L^{LW}} + \sqrt{\gamma_M^+\gamma_L^-} + \sqrt{\gamma_M^-\gamma_L^+}) \tag{4}$$

where θ is the contact angle of a liquid *L* on the membrane surface *M*, γ_L is the surface tension of the liquid, γ_M^{LW} and γ_L^{LW} are the Lifshitz-van der Waals (apolar) part of the surface tension, and γ_M^+, γ_M^-, γ_L^+ and γ_L^- describe the polar part of the surface tension (where the + and – parts are the surface tension parameters describing the electron-accepticity and electron-donaticity, respectively). Values for γ_L^{LW}, γ_L^+ and γ_L^- were taken from [32].

1.4.3.2.2 ζ-potential measurements

ζ-potential measurements were performed on the virgin SW30HRLE and Qfx SW 75ES. The measurements were executed by Anton Paar GmbH in Graz, Austria, using the zeta meter SurPASS (Anton Paar). The measuring electrolyte solutions was 10^{-3}M KCl, and the pH was adjusted by addition of high purity aqueous solutions containing NaOH or HCl. The zeta potential was calculated from the streaming potential measurements as described elsewhere [33].

1.4.3.2.3 SEM-EDX

Scanning electron microscopy with energy-dispersive X-ray spectroscopy (SEM-EDX) was performed by Fundació CTM Centre Tecnològic on the virgin TFN Qfx SW 75ES and the used TFC SW30HRLE and TFN Qfx SW 75ES. A SUPRA™ Field Emission SEM (Carl Zeiss, Germany) with a Microanalysis X-Max EDX (Oxford Instruments, United Kingdom) with INCA software was used for the imaging and analysis. The presence of N was sometimes detected (up to 4%) but was ignored in the analysis.

1.4.4 Pilots

1.4.4.1 Small scale pilot (4 inch modules)

A pilot installation designed and built by KWR Watercycle Research Institute (UAN950121) was used for the experiments with the 4 inch modules. A schematic of the set-up is provided in figure 1. The water flow through the system was regulated by two independent high pressure pumps before the membranes. The pumps were limited to a maximum pressure of about 1700 kPa. Dosing of chemicals was carried out by a Masterflex dosing pump (L/S digital standard drive model 77200-50, Masterflex, Schiedam, The Netherlands). Sampling was done using two quick connectors located on the feed side of each membrane and taps were connected at the concentrate side and permeate side of both membrane elements (4 sampling points in total). To measure the flows, two flow meters were installed (0-2000L/h Heinrichs Messtechnik GmbH, Köln, Germany) for the concentrate stream and two flow meters for the permeate stream (0-200L/h Heinrichs Messtechnik GmbH, Köln, Germany). For pressure measurements a Cerabar S PMC71 pressure meter (Endress&Hauser, Reinach, Switzerland) was used. The set-up was used both in once through or recirculation mode. In recirculation mode water was recirculated using a stainless steal tank (700 L) equipped with a stirrer and a cooling unit in order to keep the solution homogeneous and at a constant temperature.

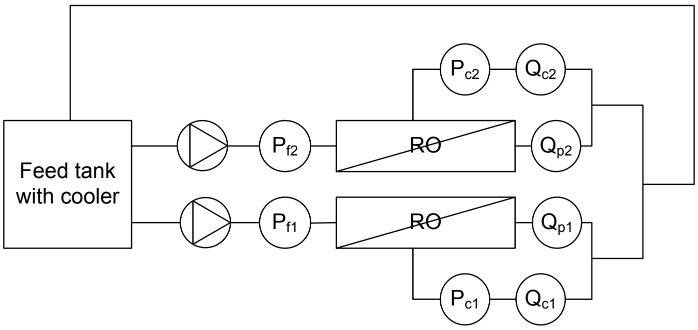

Figure 1: Schematic of the set-up used during the tests with the 4 inch modules in recirculation mode.

1.4.4.2 Full scale pilot (8 inch modules)

The large scale pilot was located in the south-west of The Netherlands, operated by Evides, and was fed with pretreated seawater from the North Sea. The pretreatment consisted of 50 µm straining, followed by optional coagulation and subsequent ultrafiltration. The SWRO pilot had five parallel pressure vessels, each containing six 8040 SWRO modules and an overall permeate production capacity of 15 m^3/h. The aforementioned system has been described in more detail elsewhere [34, 35].

The pressure vessel containing the Qfx SW 365ES elements was adapted by the installation of a separate high-pressure sampling port on its concentrate side. This enabled sampling and conductivity measurement of the concentrate of this specific pressure vessel.

1.4.5 Experiments

1.4.5.1 Small scale pilot (4 inch modules)

In the tests to determine the water and salt permeability constants (A and B, respectively - [27, 28]) and the *m* value of the TFN and TFC membranes the flux was varied from 5 to 15 L m^{-2} h^{-1} for the TFC and 5 to 30 L m^{-2} h^{-1} for the TFN membrane. For the tests to determine the *U* and *n* values the temperature was varied from 5 to 30 °C. The MTC and A were normalized to a temperature of 10 °C, the pressure drop to a feed flow of 1500 L/h and a temperature of 10 °C, and the EC passage and B to a flux of 15 L m^{-2} h^{-1} and a temperature of 10 °C. As feed water tap water filtered over a 1 µm filter was used, to which 1 g/L NaCl had been added. The tap water is produced from groundwater at water treatment plant Tull en 't Waal (Water Supply Company Vitens) by aeration and rapid sand filtration with addition of poly aluminum chloride and without post-chlorination. During tests, flow rates of the permeate and concentrate, feed and concentrate pressures, the temperature, conductivity and pH (feed, permeate, concentrate) were recorded.

In order to determine the performance of the membranes, the measured flow rates, pressures and conductivity were used to calculate trans membrane pressure (TMP), flux, membrane permeability and salt rejection – using standard equations [36].

The glycerol rejection experiments were performed with 20 mg C/L glycerol solutions, added to the previously described prefiltered tap water. The recovery in this experiment was varied from 2.4 to 8.6 % for the TFC and 2.7 to 16% for the TFN, with the flux through the membranes varying from 5 to 15 L m^{-2} h^{-1} for the TFC and 5 to 30 L m^{-2} h^{-1} for the TFN. From the obtained rejection data on glycerol rejection, the representative pore radius r_p was determined as described elsewhere by fitting the data to a membrane transport model [30, 37]. The rejection of the solute, R, as a function of the solvent flux is:

$$R = 1 - \frac{\beta \phi K_c}{1 - \left((1 - \phi K_c) \exp\left(- \frac{J_v K_c \Delta x}{K_d \varepsilon D_\infty} \right) \right)} \qquad (5)$$

where β is the hydrodynamic concentration polarization, ϕ the partition coefficient, K_c and K_d are the steric hindrance factors which depend on the ratio of the solute radius and r_p, J_v the solvent flux, and D_∞ the diffusion coefficient of the solute. Equation (5) is also the basis of traditional size exclusion based convection-diffusion models [38, 39]. The full derivation and validation of the used membrane transport model can be found elsewhere [40, 41]. The partition coefficient ϕ is given by:

$$\phi = (1 - \lambda^2) \exp(- \Delta G_i / kT) \qquad (6)$$

where $\lambda = r_p / r_s$. Note that r_p is normally used in conjunction with the ratio of membrane thickness and porosity ($\Delta x / \varepsilon$), but here the data is insufficient to obtain reliable values for both parameters for the TFC membrane. $\Delta x / \varepsilon$ was therefore fixed at 10 µm (the value that was obtained from the fit to the TFN membrane).

The pre-filtered tap water was also used for the experiments to determine the rejection of the TFC and TFN membranes for a set of pharmaceuticals (individual concentrations in the feed water of 2 µg/L, except for metformine which was spiked at a concentration of 5 µg/L) and a set of nitrosamines (individual concentrations at 1.5 µg/L). Here, the settings for the TFC and TFN membrane were a flux of 15 L m^{-2} h^{-1} and a recovery of 8 and 7%, respectively. The samples used to determine the rejection (feed and permeate) were taken after 96 hours of filtration to ensure that adsorption of the compounds to the membrane did not affect the measured rejection.

1.4.5.2 Large scale pilot (8 inch modules)

In January 2012, six virgin QuantumFlux (Qfx) SW 365ES RO membranes from NanoH$_2$O (El Segundo, California, USA) were inserted in one of the five parallel pressure vessels. The other four pressure vessels retained the original (used since 2009) SW30XHR-440i elements from Dow Filmtec. This test was terminated in July 2012, and therefore covered a period of seven months ranging in water temperature from 2-19 °C.

The pilot was operated at feed pressures (summer: 50 bar, winter: 65 bar) which resulted in a total fixed permeate production of 15 m^3/h. Cleaning in place (CIP) of the membranes was performed in the fourth week of June. The feed pressure was the same for the five pressure vessels, which resulted in a higher average flow to and recovery of the vessel containing the TFN membranes.

Flows, pressures and conductivity of feed, aggregate concentrate and aggregate permeate were measured on-line by field instrumentation. Once or twice a month, each pressure vessels' permeate discharge was isolated from the aggregate permeate header by manual manipulation of the appropriate port valves, thereby enabling measurement of individual permeate conductivity and flow. Boron concentrations in feed and permeate were determined periodically as well as by laboratory analyses. Table 3 gives the feed water quality in the period January-July 2012.

Table 3: RO feed water quality for the large scale pilot (January to end of July 2012).

parameter	minimum	average	maximum	unit
Ca	339	368	396	mg/L
Cl	17349	18490	20000	mg/L
Mg	1088	1200	1314	mg/L
Na	8759	9803	10950	mg/L
Sulphate	2418	2528	2617	mg/L
B	3.3	4.2	4.8	mg/L
pH	7.7	7.9	8.2	-

TDS	32454	32906	33270	mg/L

1.5 Results and discussion

1.5.1 Membrane characterization

1.5.1.1 Contact angle measurements

The contact angle of the active membrane layer for MilliQ, glycerol and diiodomethane of the different membranes were determined. Based on the measured contact angles with MilliQ, it appears that the virgin and used TFN are more hydrophobic than the TFC, and with usage their hydrophilicity increases slightly (Table 4). The γ_M^+ of the virgin and fouled TFN are somewhat higher than that of the TFC. The γ_M^- of the virgin and fouled TFN are lower than that of the TFC. The ΔG_i for glycerol is positive for both TFN and TFC, but clearly higher for the TFN. Thus it is more difficult for glycerol to pass the TFC than the TFN. Also, the used membranes show a higher resistance to passage of glycerol than the virgin membranes.

Table 4: Membrane contact angle, surface tension and ΔG.

	θ (°)			γ (mJ/m²)			ΔG_i for glycerol (*10^{-21} J)
	MilliQ	glycerol	diiodomethane	γ_M^{LW}	γ_M^+	γ_M^-	
TFN virgin	53±3	52±4	42±5	38	0.6	26	1.1
TFN used	37±7	37±8	39±3	39	1.5	36	1.3
TFC virgin	43±4	48±3	30±4	43	0.2	36	1.5
TFC used	24±3	32±5	13±3	48	0.5	44	1.6

1.5.1.2 ζ-potential measurements

The ζ-potential of the TFC and TFN membranes were determined (figure 2). The ζ-potential of the TFC (SW30HRLE) is very similar to those previously published for this type of SWRO membrane [23, 25]. The plateau-value of the ζ-potential for the TFC is reached around pH 6, and the iso-electric point (iep) is around pH 3. The ζ-potential of the TFN is indistinguishable from that of the TFC. Since both membranes have a polyamide thin film, this is perhaps not very surprising. The nanoparticles probably have a different ζ-potential and iep, but do not appear to affect the ζ-potential of the TFN membrane.

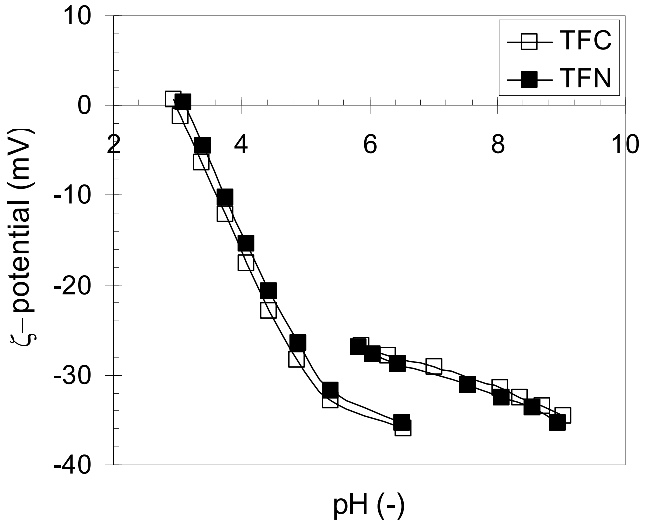

Figure 2: ζ-potentials of the TFC (SW30HRLE) and TFN (Qfx SW 75ES) as a function of pH. Measurements were performed in a 1 mM KCl solution, in two series (pH 6 to 9 with NaOH, and pH 6.5 to 3 with HCl).

1.5.1.3 SEM-EDX

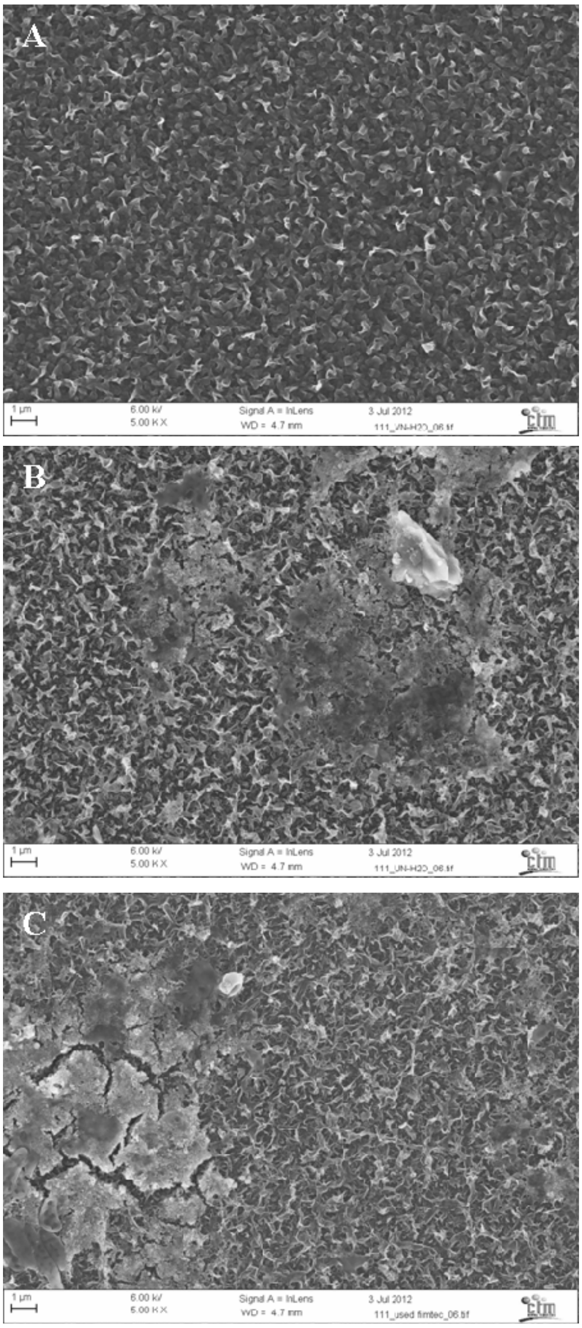

Figure 3: SEM image of a) the virgin TFN (Qfx SW 75ES), b) the used TFN and c) the used TFC (SW30HRLE) – top view. Scalebar (bottom left of pictures) represents 1 µm.

SEM-EDX analysis of the virgin TFN (figure 3) and the used (lightly fouled) TFN and TFC were made. The virgin TFC (SW30HRLE) was not analyzed as such, as this membrane has already been analyzed by SEM before [23]. SEM-EDX analysis was performed on a clean part of the used TFC (figure 3). The SEM image of the membrane layer of the virgin TFN shows the peak-and-valley structure, which are attributed to the top facial polyamide layers of several hundred nanometers thick which are generally observed for polyamide thin films [23, 44]. Generally, in the SEM-EDX analysis of virgin TFC membranes with a 0.2 µm thick active membrane layer of cross-linked polymer, the elemental composition found is that of the much thicker microporous layer beneath. This is because the penetration depth of the X-rays is in the order of several microns. Here, for the TFN the composition detected with EDX is also mainly from the microporous layer and gives the atomic composition as 80% C, 16% O and

3% S. For the clean part of the TFC the EDX gives an atomic composition of 80% C, 17% O and 3% S, which is close to the expected composition of a polysulfone support layer (84% C, 13% O, 3% S). Interestingly, the presence of the nanoparticles in the TFN is not detected. If we assume the nanoparticles are zeolites ($Na_{12}Al_{12}Si_{12}O_{48} \cdot 27H_2O$), that the detection limit for Na, Al, or Si is about 0.1 wt% and that the thin film of about 100-200 nm only represents 10% of the total volume detected with EDX (penetration depth 1-2 µm), the presence of zeolites (about 17 wt% each of Na, Si and Al) should be detected if it is above 6 wt%. The fact that no elements besides C, O and S are detected suggests that the inorganic nanoparticles are present in a minor amount (6 wt% at most).

The tests were performed with tap water filtered over a 1 µm filter. However, some small particles (colloids composed mostly of iron oxides) and DOC (2 mg/L) still remain in the tap water [45] and thus, some colloidal fouling and adsorption of DOC can still occur. The recovery was generally very low, so it is expected that the solubility of salts was not exceeded and that no scaling occurred.

The used membranes showed only a small amount of fouling: no impact was observed over the course of the experiments that indicated a decline in the permeability, but some fouling can be seen in the SEM pictures (figure 3). EDX analysis of the fouled parts of the membranes showed that both membranes were fouled by small amounts of Fe (3% detected) and extra O (C/O ratio dropped from about 5 to 1.5). Trace amounts (<0.5%) of other atoms were also detected, most notably Al, P and Si. The feed water contains colloids composed of iron oxide and aluminium oxide [45] and these particles lightly fouled the membranes during the tests.

1.5.2 Small pilot scale evaluation (4 inch modules)

1.5.2.1 Permeability and normalization

The flux as a function of pressure was determined simultaneously for both the TFC and the TFN membrane with tap water with 1 g/L NaCl, at applied pressures (feed pressure, P_f) of 300 to 1700 kPa. The water permeability was calculated from the measured flux and is $(2.4 \pm 0.1) \cdot 10^{-12}$ m s^{-1} Pa^{-1} (average and standard deviation) for the TFC and $(4.6 \pm 0.3) \cdot 10^{-12}$ m s^{-1} Pa^{-1} for the TFN. The TFN was expected on the basis of the manufacturer’s information to have a 1.8 higher permeability than the TFC, and here we find a factor of 1.9.

A, the water permeability constant, and B, the salt (NaCl) permeability constant, were also determined and found to be in the normal range (see table 5) [46]. A is nearly twice as big for the TFN membrane compared to the TFC. The B values for the TFN and TFC are nearly equal, although it is slightly higher for the TFN compared to the TFC.

U, *n* and *m* values of both TFN and TFC were determined as well (table 5). As expressed by *U*, the temperature has less influence on the permeability for water for the TFN then for the TFC. The *n* value of the TFN is smaller than that of the TFC, showing that the ΔP of the TFN is less sensitive to changes in the temperature. The *m* values are within error for both membranes.

Table 5: Overview of determined constants for both membranes.

membrane	A (L m^{-2} h^{-1} bar^{-1})	B (L m^{-2} h^{-1})	A/B	*U*	*n*	*m*
TFN	1.7±0.1	0.06±0.01	29	2890	0.30	1.24
TFC	0.9±0.1	0.05±0.02	17	3350	0.25	1.22

Average±standard deviation. A and B factors were calculated from the experiments with a flux of 15 L m^{-2} h^{-1} and normalized.

1.5.2.2 Rejection

The electrical conductivity (EC) was measured for the feed, concentrate and permeate of both the TFC and the TFN membrane. The EC rejection was calculated and increases with increasing P_f (figure 4), as expected as the water flux depends mostly on the pressure difference but the salt flux depends mostly on the concentration difference before and after the membrane. The salt rejection increases with higher P_f and higher flux through the membranes (see figure 4). The normalized EC rejection is 99.7±1.0% for the TFC and 99.6±0.1% for the TFN. This value is very close to the stabilized salt rejection given by the manufacturers. The EC rejection of the TFN seems to be slightly higher than that of the TFC, at the same P_f.

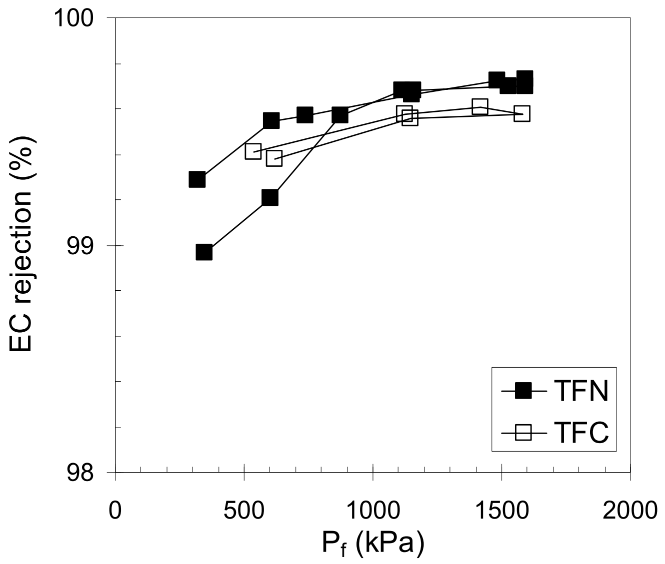

Figure 4: Measured EC rejection as a function of P_f for the TFN and TFC membranes.

Besides the EC rejection, the rejection for glycerol was determined as well. In these tests the permeability for the TFC and TFN were (2.5±0.1)*10^{-12} m s^{-1} Pa^{-1} and (4.8±0.1)*10^{-12} m s^{-1} Pa^{-1}, respectively. The EC rejection for the TFC and TFN were 99.6±0.2% and 99.4±0.3%, respectively. These are nearly the same values as in the experiments to determine the water and salt permeability described in the previous paragraph. The glycerol rejection of the TFC and TFN membranes increase with increasing flux and are generally high (>97%, figure 5), especially at higher fluxes (>98.5% at a flux of 15 L m^{-2} h^{-1} or higher). The TFC seems to have a slightly higher rejection (about 0.5%) for glycerol than the TFN. Fitting this data to the membrane transport model resulted in r_p values of 0.21 and 0.22 nm for the TFC and TFN, respectively. These values are lower than those found for nanofiltration membranes elsewhere [30, 37], which seems reasonable.

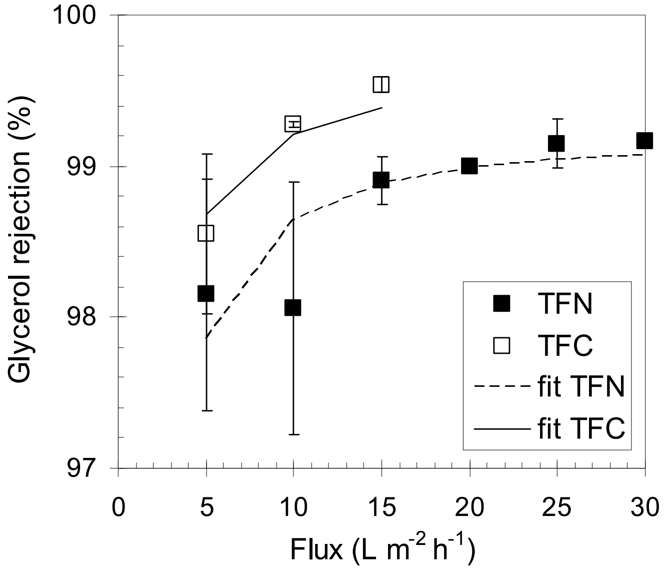

Figure 5: Glycerol rejection and fits to the rejection of the TFC and TFN membranes as a function of the flux. The error bars give the standard deviation of the measurements.

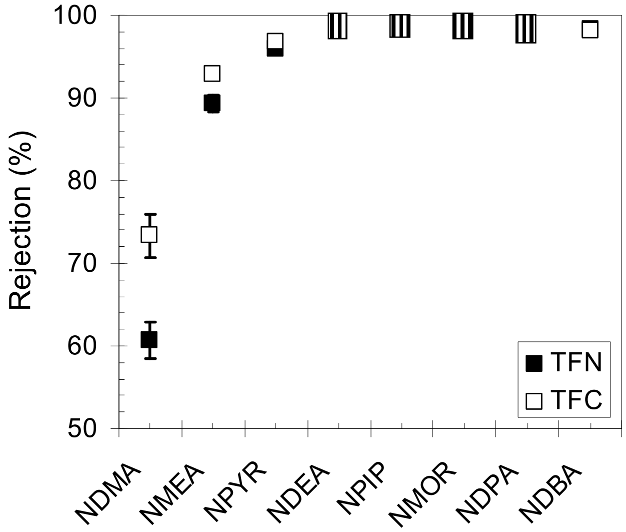

Figure 6: Rejection of the TFC and TFN membranes for various nitrosamines. The nitrosamines are ordered in increasing MW from left to right. The error bars give the standard deviation of the measurements. For NDEA, NPIP, NMOR and NDPA the rejection values as determined were limited by the LOQ and therefore only determined as larger then. They are therefore shown as bars with black and white stripes.

The rejection for the nitrosamines for both membranes was determined as well, and is in general good (>90%, see figure 6). There is a clear correlation between the molecular weight or size of the nitrosamine and the rejection for small nitrosamines. The smallest, NDMA with a molecular weight (MW) of 74.1 g/mol, shows the lowest rejection. The second smallest, NMEA (MW= 88.1 g/mol), shows the second lowest rejection. The third smallest, NPYR (MW= 100 g/mol), shows the third lowest rejection. Also, for these three nitrosamines, the rejection is lower for the TFN than for the TFC. For the other nitrosamines the determined rejection was limited by the LOQ, except for NDBA which had a relatively low LOQ. The rejection for NDBA is 98.1±0.1% for the TFN and 98.3±0.1% for the TFC – again showing that the TFC has a slightly higher rejection for nitrosamines than the TFN. However, both TFN and TFC membranes are a very good barrier (factor 10 to >50 removal) for nitrosamines, except for NDMA.

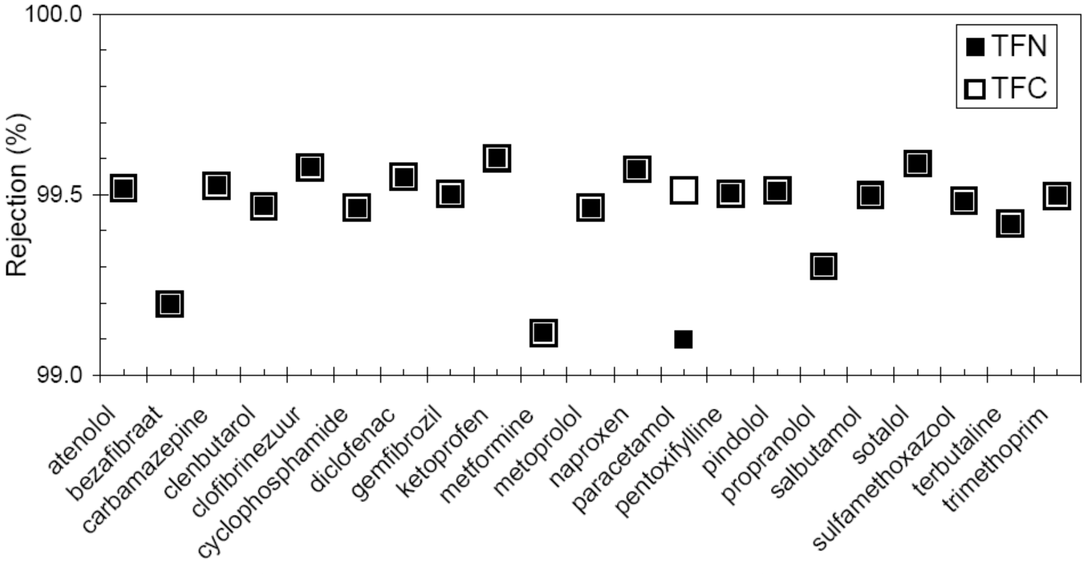

Figure 7: Rejection of the TFC and TFN membranes for various pharmaceuticals. Note that when the rejection of the TFN and TFC is the same, the value is limited by the limit of quantification.

The rejection for the pharmaceuticals was in all cases but one above the determinable limit (figure 7), which was limited by the limit of quantification of the detection method. For the TFN paracetamol was removed to an extent that was still above the limit of quantification, resulting in a determined rejection of 99.1% for the TFN. As far as could be determined, again the rejection of the TFN is lower than that of the TFC – as was the case for glycerol and the nitrosamines. However, both TFN and TFC are an excellent barrier (factor 100 to >200 removal) for the tested pharmaceuticals.

1.5.2.3 Comparison of TFC and TFN

The virgin TFC and TFN share similarities in the structure of the active membrane layer. The atomic composition of the TFC and TFN are different, most notably the presence of 4% N in the TFN which is absent in the TFC. The TFN is stated to contain inorganic nanoparticles [9] which were not detected with EDX. Also the ζ-potential and iep of both membranes are the same. The TFC is slightly more hydrophilic than the TFN.

The TFN outperforms the TFC as the water permeability is a factor of two higher allowing for a factor two higher water production. The measured EC rejection is similar for both membranes, although the normalized EC rejection is slightly higher for the TFC compared to the TFN. Finally, the TFC shows a higher rejection for low molecular weight compounds (glycerol, several nitrosamines including NDMA, paracetamol) than the TFN, at the same flux. At the same applied pressure however, the observed differences in rejection of low molecular weight compounds would be smaller.

1.5.3 Large pilot scale evaluation (8 inch modules)

The performance of the TFN and TFC membranes in the large scale pilot was more difficult to compare because the TFC membranes were already in operation from January 2009 onwards. Hence, the comparison presented below pertains to *aged* TFC with *virgin* TNF. The performance of the TFC membranes had changed significantly (about 30% drop in the membrane transfer coefficient) during three years of operation.

Note that a different type of TFC membrane was used in the tests with the large pilot installation (Filmtec SW30XHR-440i) than in the smaller scale pilot installation (Filmtec SW30HRLE 4040).

1.5.3.1 Flux

Long term tests at a total permeate production of 15 m^3/h and varying temperatures (2-18 °C) and feed pressure (50-65 bar) in a large scale pilot installation showed that the virgin TFN membrane had a higher flux (at the same feed pressure) than the aged TFC membrane (figure 8A). On average the flux of the virgin TFN was 1.8±0.2 times higher than that of the aged TFC. The difference between the two membranes was largest at lower temperatures and pressures.

1.5.3.2 Salt rejection

The EC rejection of the virgin TFN and aged TFC was calculated from the EC in the feed, at the same time and in the same circumstances as the flux (figure 8B). On average the EC passage of the virgin TFN (0.7±0.2%) was 1.5±0.3 times higher than that of the aged TFC (0.5±0.2%). Again, the difference between the two membranes was largest at lower temperatures and pressures. After the CIP, there was a peak in salt passage for both types of membranes. The TFN had a higher recovery than the aged TFC and therefore a higher average EC in the feed side of the membranes in the pressure vessel. Calculating the EC passage for the average EC results in an EC passage of 0.54% for the TFN and 0.41% for the aged TFC. The reported values for stabilized salt passage from standardized tests (25 °C, pH 8, 32000 ppm NaCl, 5 ppm boron, 8% recovery) are lower, being 0.3% for both the TFN and TFC [47, 48].

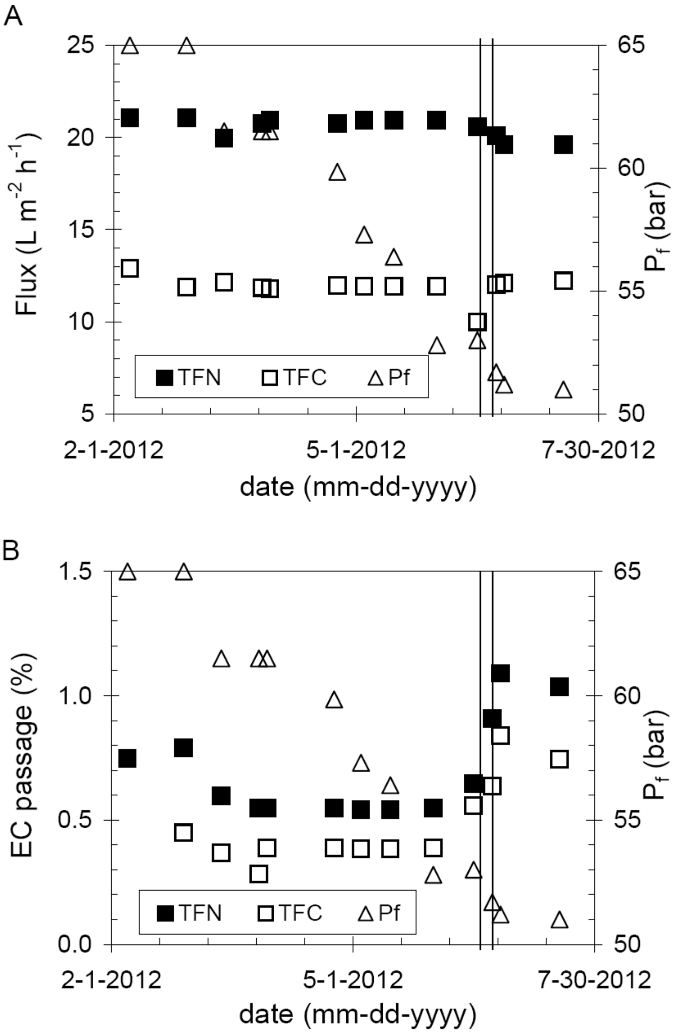

Figure 8: EC passage and flux of the virgin TFN and aged TFC membranes in the larger scale pilot. A) Flux as a function of time. B) EC passage as a function of time. P_f is given as well, as are the two times cleaning in place was performed (vertical lines).

1.5.3.3 Boron rejection

The boron concentration in the permeate of the pressure vessels containing the virgin TFN and aged TFC membranes was determined throughout the whole testing period (January 2012 to July 2012). The boron concentration in the permeate increases with the temperature of the feed water (figure 9). On average the boron concentration in the permeate for the TFC was 0.53±0.17 mg/L and for TFN 1.2±0.4 mg/L. Thus, the observed average boron rejection calculated on the boron concentration in the feed and permeate was 71±4% and 87±8% for the TFN and aged TFC, respectively. Again, as the pressure vessel with the TFN membranes was run at a higher recovery we can calculate the boron removal based on the average boron concentration in the feed side of the membranes in the pressure vessel, which was 78 and 89% for the TFN and TFC, respectively. In both cases the boron rejection in the large scale pilot plant are below the values obtained in standardized tests by the manufacturer, being 89 and 93% for the TFN and TFC, respectively [47, 48].

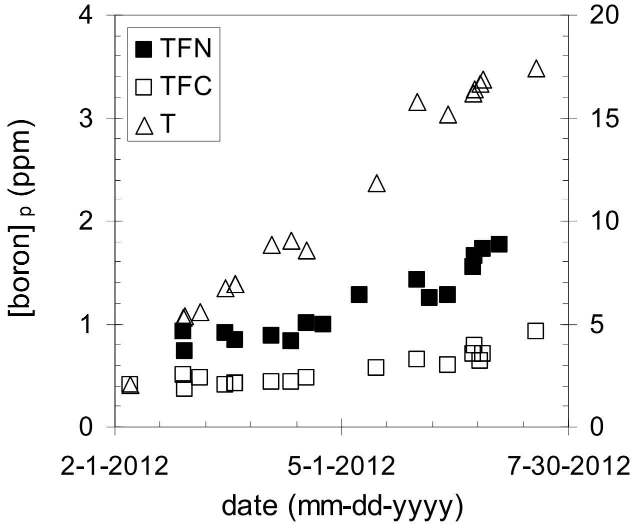

Figure 9: Boron concentration in the permeate of the pressure vessel(s) containing virgin TFN or aged TFC membranes, and the corresponding temperature of the feed water.

1.5.4 Overall comparison and outlook

The TFN membrane shows a higher flux than the TFCs (SW30HRLE and aged SW30XHR) in flux, at similar salt rejections (slightly lower salt rejection found for SW30HRLE and slightly higher salt rejection found for aged SW30XHR). However, the rejection of small organic molecules (glycerol, NDMA) of the TFN is lower than that of the TFC (SW30HRLE). The rejection of boron in seawater desalination of the TFN is lower than that of the aged TFC (SW30XHR). It has been observed that in general a lower boron removal is reached in full scale seawater desalination installations (around 65-85% in the USA) than the reported values from standardized test [10]. Seawater usually contains about 4-5 mg/L of boron. The removal of boron that is required for a single pass installation to produce drinking water depends on the health norm. California and the EU have a guideline value for boron in drinking water of 1 mg/L [12, 13], whereas the WHO guideline is 2.4 mg/L [14]. A boron removal of about 50% is sufficient where the WHO norm applies, but 80% is needed in California and the EU. In the large scale pilot, both TFN and TFC showed a sufficiently high boron rejection to comply with the WHO guideline within a single pass, but only the TFC (SW30XHR) showed a high enough boron rejection (80-90%) during the whole period of the trial that complies with the more stringent guidelines from California and the EU. This means that the potential savings obtained by using the higher flux TFN tested here (being a smaller installation and/or savings in energy) could be offset by the need for a second pass – or other measures – if the boron concentration in the finished product needs to be low.

NanoH$_2$O recently launched two new TFN membranes with a higher boron rejection, but with decreased water permeability [9] (compared to the TFN tested here). Unfortunately, this brings the water permeability to the level of the TFC membranes tested here. Further optimization of the TFN seems to be needed in order for TFNs to outperform the current generation of TFCs, when regulations for boron levels in the finished product are strict.

Finally, it seems that the added inorganic nanoparticles in the TFN membrane do not affect the performance significantly, which is perhaps not very surprising as they are porobably present on a low amount (<6 wt% in the active membrane layer). In the scientific literature, the mechanism by which zeolite particles embedded in TFN membranes are supposed to increase the permeability has not been determined yet, although it has been suggested that defects and molecular sieving largely govern transport through this types of TFN membranes [7, 8]. A study directly comparing TFC and TFN membranes with more similar water permeability and equal active membrane layer thickness would be needed to substantiate the hypothesis that a low amount of nanoparticles in fact does not change the properties of the membrane significantly.

1.6 Conclusions

Pilot scale experiments with 4 inch SWRO modules show that the TFN's water permeability is a factor of two higher than that of the TFC. The EC passage is similar for both membranes (shown by the nearly similar salt permeability constants). Finally, the TFC shows a higher rejection of low molecular weight nitrosamines than the TFN (at the same flux).
A larger scale pilot test (with parallel pressure vessels containing six full scale elements) from January to July 2012 confirmed the higher flux of the TFNs compared to the TFCs membranes. However, the EC passage of the TFNs was about 40% higher than that of the aged TFCs. Finally, the boron concentration in the permeate of the TFC membranes complied with the more stringent norms (1 mg/L boron allowed) all of the time, whereas the boron concentration in the permeate of the TFN membrane only did so a part of the time (i.e. winter/low water temperature season).

1.7 Acknowledgements

This research was conducted in the framework of the Joint Research Program (BTO) of the Dutch drinking water companies. A.R.D. Verliefde (TU Delft, Ghent University) is thanked for his contribution to the model calculations to determine the representative pore radius. The TU Delft is thanked for providing access to perform contact angle measurements. G. Ribera Simon and I. Gonzalez (both from Fundació CTM Centre Tecnològic, Barcelona, Spain) are thanked for arranging and performing the SEM-EDX analysis. S. Zierler (Anton Paar, Graz, Austria) is thanked for performing the ζ-potential measurements.

1.8 List of symbols and abbreviations

a – actual
A – the water permeability constant
AFM – atomic force microscopy
B – the salt (NaCl) permeability constant
c – concentrate
CI – chemical ionization
CIP – Cleaning in place
D_∞ – the diffusion coefficient of the solute
EC – electrical conductivity
f – feed
GC-MS – gas chromatography combined with mass spectrometry
HILIC – hydrophilic interaction chromatography
ICP-MS – inductively coupled plasma mass spectrometry
iep – iso-electric point
J_v – the solvent flux
K_c and K_d – the steric hindrance factors which depend on the ratio of the solute radius and r_p
L – liquid
LOQ – limit of quantification
m – the correction factor for the flow effects on ΔP
M – membrane
n – the correction factor for the temperature effect on ΔP
NDBA – N-nitroso-n-dibutylamine
NDEA – N- nitrosodiethylamine
NDMA – N-nitrosodimethylamine
NDPA – N-nitrosodi-n-propylamine
NF – nanofiltration
NMEA – N-nitrosomethylethylamine
NMOR – N-nitrosomorpholine
NPIP – N-nitrosopiperidine
NPOC – non purgeable organic carbon
NPYR – N-nitrosopyrrolidine
p – permeate
P_f – feed pressure
Q – flow

QCF – capacity correction factor
Qfx – QuantumFlux
r – reference
r_p – the representative pore radius
R – rejection of a solute
RP – reversed phase
RMS – root mean squared
RO – reverse osmosis
S – solute
SEM-EDX – scanning electron microscopy with energy-dispersive X-ray spectroscopy
SPE – solid phase extraction
SWRO – seawater reverse osmosis
T – temperature
TCF – temperature correction factor
TDS – total dissolved solids
TFC – thin film composite (in this study either Filmtec SW30XHR-440i or Filmtec SW30HRLE 4040)
TFN – thin film nanocomposite (in this study either Qfx SW 75ES RO or Qfx SW 365ES RO)
TMP – trans membrane pressure
U – the correction factor for the temperature effect on the mass transfer coefficient K_w
UPLC-MS/MS – ultra performance liquid chromatography coupled with a mass spectrometer
WHO – World Health Organization
β – the hydrodynamic concentration polarization
ΔG_{SLM} – the free energy of interaction, per unit area, between the solute and the membrane in a liquid
ΔP – pressure drop
$\Delta x/\varepsilon$ – the ratio of membrane thickness and porosity
η – viscosity
γ – surface tension
γ^{LW} – the surface tension parameter describing the apolar (Lifshitz-van der Waals) component
γ^{+} – the surface tension parameter describing the electron-accepticity
γ^{-} – the surface tension parameter describing the electron-donaticity
ϕ – the partition coefficient
θ – contact angle

1.9 References

[1] K.P. Lee, T.C. Arnot, D. Mattia, A review of reverse osmosis membrane materials for desalination--Development to date and future potential, Journal of Membrane Science, 370 (2011) 1-22.
[2] B.H. Jeong, E.M.V. Hoek, Y.S. Yan, A. Subramani, X.F. Huang, G. Hurwitz, A.K. Ghosh, A. Jawor, Interfacial polymerization of thin film nanocomposites: A new concept for reverse osmosis membranes, Journal of Membrane Science, 294 (2007) 1-7.
[3] C.J. Kurth, R. Burk, J. Green, Utilizing nanotechnology to enhance RO membrane performance for seawater desalination, in: IDA World Congress, Perth, Australia, 2011, pp. PER11-323.
[4] R.R. Nair, H.A. Wu, P.N. Jayaram, I.V. Grigorieva, A.K. Geim, Unimpeded Permeation of Water Through Helium-Leak–Tight Graphene-Based Membranes, Science, 27 (2012) 442-444.
[5] J.K. Holt, H.G. Park, Y.M. Wang, M. Stadermann, A.B. Artyukhin, C.P. Grigoropoulos, A. Noy, O. Bakajin, Fast mass transport through sub-2-nanometer carbon nanotubes, Science, 312 (2006) 1034-1037.
[6] M. Kumar, M. Grzelakowski, J. Zilles, M. Clark, W. Meier, Highly permeable polymeric membranes based on the incorporation of the functional water channel protein Aquaporin Z, Proceedings of the National Academy of Sciences of the United States of America, 104 (2007) 20719-20724.
[7] M.L. Lind, A.K. Ghosh, A. Jawor, X. Huang, W. Hou, Y. Yang, E.M.V. Hoek, Influence of zeolite crystal size on zeolite-polyamide thin film nanocomposite membranes, Langmuir, 25 (2009) 10139-10145.
[8] M.L. Lind, D.E. Suk, T.V. Nguyen, E.M.V. Hoek, Tailoring the structure of thin film nanocomposite membranes to achieve seawater RO membrane performance, Environmental Science and Technology, 44 (2010) 8230-8235.
[9] www.nanoh2o.com, in.

[10] J. Kim, M. Wilf, J.-S. Park, J. Brown, Boron Rejection By Reverse Osmosis Membranes: National Reconnaissance
And Mechanism Study, in: Desalination and water purification research (DWPR), U.S. Department of the Interior, Bureau of Reclamation, 2009.
[11] K.L. Tu, L.D. Nghiem, A.R. Chivas, Boron removal by reverse osmosis membranes in seawater desalination applications, Separation and Purification Technology, 75 (2010) 87-101.
[12] Council Directive 98/83/EC of 3 November 1998 on the quality of water intended for human consumption Official Journal of the European Union: Legislation, 330 32–54.
[13]
http://www.cdph.ca.gov/certlic/drinkingwater/Documents/Notificationlevels/notificationlevels.pdf, 2010, in.
[14] WHO, Guidelines for Drinking-water Quality, Fourth Edition, WHO, 2011.
[15] D. Fatta-Kassinos, S. Meric, A. Nikolaou, Pharmaceutical residues in environmental waters and wastewater: Current state of knowledge and future research, Analytical and Bioanalytical Chemistry, 399 (2011) 251-275.
[16] T. Heberer, Occurrence, fate, and removal of pharmaceutical residues in the aquatic environment: A review of recent research data, Toxicology Letters, 131 (2002) 5-17.
[17] O.A. Jones, J.N. Lester, N. Voulvoulis, Pharmaceuticals: A threat to drinking water?, Trends in Biotechnology, 23 (2005) 163-167.
[18] K.M. Onesios, J.T. Yu, E.J. Bouwer, Biodegradation and removal of pharmaceuticals and personal care products in treatment systems: A review, Biodegradation, 20 (2009) 441-466.
[19] M. Klavarioti, D. Mantzavinos, D. Kassinos, Removal of residual pharmaceuticals from aqueous systems by advanced oxidation processes, Environment International, 35 (2009) 402-417.
[20] M. Petrovic, M.J.L. De Alda, S. Diaz-Cruz, C. Postigo, J. Radjenovic, M. Gros, D. Barcelo, Fate and removal of pharmaceuticals and illicit drugs in conventional and membrane bioreactor wastewater treatment plants and by riverbank filtration, Philosophical Transactions of the Royal Society A: Mathematical, Physical and Engineering Sciences, 367 (2009) 3979-4003.
[21] C. Bellona, J.E. Drewes, P. Xu, G. Amy, Factors affecting the rejection of organic solutes during NF/RO treatment - A literature review, Water Research, 38 (2004) 2795-2809.
[22] K.V. Plakas, A.J. Karabelas, Removal of pesticides from water by NF and RO membranes - A review, Desalination, 287 (2012) 255-265.
[23] W. Lee, C.H. Ahn, S. Hong, S. Kim, S. Lee, Y. Baek, J. Yoon, Evaluation of surface properties of reverse osmosis membranes on the initial biofouling stages under no filtration condition, Journal of Membrane Science, 351 (2010) 112-122.
[24] H. Hyung, J.H. Kim, A mechanistic study on boron rejection by sea water reverse osmosis membranes, Journal of Membrane Science, 286 (2006) 269-278.
[25] C.Y. Tang, Y.N. Kwon, J.O. Leckie, Probing the nano- and micro-scales of reverse osmosis membranes-A comprehensive characterization of physiochemical properties of uncoated and coated membranes by XPS, TEM, ATR-FTIR, and streaming potential measurements, Journal of Membrane Science, 287 (2007) 146-156.
[26] C.Y. Tang, Y.-N. Kwon, J.O. Leckie, Effect of membrane chemistry and coating layer on physiochemical properties of thin film composite polyamide RO and NF membranes: II. Membrane physiochemical properties and their dependence on polyamide and coating layers, Desalination, 242 (2009) 168-182.
[27] J.G. Wijmans, R.W. Baker, The solution-diffusion model: A review, Journal of Membrane Science, 107 (1995) 1-21.
[28] S. Loeb, L. Titelman, E. Korngold, J. Freiman, Effect of porous support fabric on osmosis through a Loeb-Sourirajan type asymmetric membrane, Journal of Membrane Science, 129 (1997) 243-249.
[29] R. Rautenbach, R. Albrecht, Membrane Processes, John Wiley & Sons Inc., New York, 1989.
[30] A.R.D. Verliefde, E.R. Cornelissen, S.G.J. Heijman, E.M.V. Hoek, G.L. Amy, B. Van Der Bruggen, J.C. Van Dijk, Influence of solute-membrane affinity on rejection of uncharged organic solutes by nanofiltration membranes, Environmental Science and Technology, 43 (2009) 2400-2406.
[31] C.J. van Oss, Development and applications of the interfacial tension between water and organic or biological surfaces, Colloids and Surfaces B: Biointerfaces, 54 (2007) 2-9.
[32] J.J. Jasper, The Surface Tension of Pure Liquid Compounds, Journal of Physical and Chemical Reference Data 1(1972) 841-1009.

[33] M. Wegmann, B. Michen, T. Luxbacher, J. Fritsch, T. Graule, Modification of ceramic microfilters with colloidal zirconia to promote the adsorption of viruses from water, Water Research, 42 (2008) 1726-1734.
[34] A. Alhadidi, A.J.B. Kemperman, R. Schurer, J.C. Schippers, M. Wessling, W.G.J. Van der Meer, Using SDI, SDI + and MFI to evaluate fouling in a UF/RO desalination pilot plant, Desalination, 285 (2012) 153-162.
[35] R. Schurer, A. Janssen, L. Villacorte, M. Kennedy, Performance of ultrafiltration and coagulation in an Uf-RO seawater desalination demonstration plant, Desalination and Water Treatment, 42 (2012) 57-64.
[36] M. Mulder, Basic principles of membrane technology, 2nd ed., Kluwer Academic Publishers, 1996.
[37] S. Botton, A.R.D. Verliefde, N.T. Quach, E.R. Cornelissen, Influence of biofouling on pharmaceuticals rejection in NF membrane filtration, Water Research, 46 (2012) 5848-5860.
[38] W.R. Bowen, A.W. Mohammad, N. Hilal, Characterisation of nanofiltration membranes for predictive purposes - Use of salts, uncharged solutes and atomic force microscopy, Journal of Membrane Science, 126 (1997) 91-105.
[39] L.D. Nghiem, A.I. Schäfer, M. Elimelech, Removal of Natural Hormones by Nanofiltration Membranes: Measurement, Modeling and Mechanisms, Environmental Science and Technology, 38 (2004) 1888-1896.
[40] A.R.D. Verliefde, E.R. Cornelissen, S.G.J. Heijman, J. Verberk, G.L. Amy, B. Van der Bruggen, J.C. van Dijk, The role of electrostatic interactions on the rejection of organic solutes in aqueous solutions with nanofiltration, Journal of Membrane Science, 322 (2008) 52-66.
[41] A.R.D. Verliefde, E.R. Cornelissen, S.G.J. Heijman, J.Q.J.C. Verberk, G.L. Amy, B. Van der Bruggen, J.C. van Dijk, Construction and validation of a full-scale model for rejection of organic micropollutants by NF membranes, Journal of Membrane Science, 339 (2009) 10-20.
[42] V. Nikolakis, Understanding interactions in zeolite colloidal suspensions: A review, Current Opinion in Colloid and Interface Science, 10 (2005) 203-210.
[43] C.P. Huang, E.A. Rhoads, Adsorption of Zn(II) onto hydrous aluminosilicates, Journal of Colloid and Interface Science, 131 (1989) 289-306.
[44] V. Freger, Nanoscale heterogeneity of polyamide membranes formed by interfacial polymerization, Langmuir, 19 (2003) 4791-4797.
[45] S. Salvador Cob, C. Beaupin, B. Hofs, M.M. Nederlof, D.J.H. Harmsen, E.R. Cornelissen, A. Zwijnenburg, F.E. Genceli Güner, G.J. Witkamp, Silica and silicate precipitation as limiting factors in high-recovery reverse osmosis operations, Journal of Membrane Science, 423–424 (2012) 1-10.
[46] M.J. Kotelyanskii, N.J. Wagner, M.E. Paulaitis, Atomistic simulation of water and salt transport in the reverse osmosis membrane FT-30, Journal of Membrane Science, 139 (1998) 1-16.
[47] http://www.nanoh2o.com/products/qfx-sw-365-es, in.
[48] http://www.dowwaterandprocess.com/products/membranes/sw30xhr_440i.htm, in.